Dinuclear and Dendritic Polynuclear Ruthenium(II) and Osmium(II) Polypyridine Complexes: Electrochemistry at Very Positive Potentials in Liquid SO_2

Paola Ceroni,[†] Francesco Paolucci,[†] Carmen Paradisi,[†] Alberto Juris,[†] Sergio Roffia,*[,†,‡] Scolastica Serroni,[§] Sebastiano Campagna,[§] and Allen J. Bard*[,⊥,∥]

Contribution from the Dipartimento di Chimica "G. Ciamician", Università di Bologna, via Selmi 2, 40126 Bologna, Italy, Dipartimento di Chimica Inorganica, Chimica Analitica e Chimica Fisica, Università di Messina, Via Sperone 31, 98166 Messina, Italy, and Department of Chemistry and Biochemistry, The University of Texas at Austin, Austin, Texas 78712

Received January 2, 1998

Abstract: The electrochemistry in liquid SO_2 of Ru^{II} and Os^{II} dendritic polynuclear complexes (two hexanuclear species, having as the core a bis-chelating ligand, and one decanuclear species, built around a metal core) has been performed together with that of several of their lower-nuclearity analogues (five dinuclear and one trinuclear species), which can be considered as components of the larger dendritic species. All of the compounds contain 2,3- or 2,5-bis(2-pyridyl)pyrazine (2,3- or 2,5-dpp) as bridging ligands and 2,2′-bipyridine (bpy) as terminal ligands. The identification of the redox sites for the compounds with high nuclearity was made possible by a bottom-up approach based on an extensive comparison of their electrochemical behavior with that of the simpler species. Owing to the large anodic potential window of liquid SO_2 (to ~4.3 V vs SCE under our experimental conditions) in conjunction with tetrabutylammonium hexafluoroarsenate as supporting electrolyte, several metal- and ligand-centered oxidations not previously observed for these compounds are reported. In particular, we observed (i) the second oxidation of Os ions (Os^{III}/Os^{IV}), (ii) the inner Ru ion oxidations (Ru^{II}/Ru^{III}) for complexes with higher-than-2 nuclearity (reported for the first time in dendrimers), and (iii) bpy and dpp oxidation. Metal−metal interaction in the Os dinuclear compound, inferred from the electrochemical data, depends on the oxidation state of the metals. For the two investigated hexanuclear compounds, $\{[(bpy)_2Ru(\mu\text{-}2,3\text{-}dpp)]_2Ru(\mu\text{-}2,3\text{-}dpp)Ru[(\mu\text{-}2,3\text{-}dpp)Ru(bpy)_2]_2\}^{12+}$ and $\{[(bpy)_2Ru(\mu\text{-}2,3\text{-}dpp)]_2Ru(\mu\text{-}2,5\text{-}dpp)Ru[(\mu\text{-}2,3\text{-}dpp)Ru(bpy)_2]_2\}^{12+}$, two sets of electrochemically equivalent Ru ions were found: the four external Ru ions give rise to a four-electron-transfer peak, and the two internal Ru ions correspond to a bielectronic peak. The decanuclear compound $[Ru\{(\mu\text{-}2,3\text{-}dpp)Ru[(\mu\text{-}2,3\text{-}dpp)Ru(bpy)_2]_2\}_3]^{20+}$ presents three sets of Ru-based oxidations: a six-electron process due to the oxidation of the six peripheral Ru centers, a one-electron process assigned to the central metal, and a three-electron process involving oxidation of the three intermediate metal centers. The location of ligand oxidation on a bridge or a terminal bpy identifies the easier-to-oxidize ligand and gives information about the electronic distribution in the complex.

Introduction

In the past few years there has been an increasing interest in the synthesis and properties of dendrimers.[1] In particular, dendrimers based on polynuclear metal complexes have been extensively studied[2] for both fundamental and applicative reasons. For example, if the metal-based dendrimers are made of photo- and redox-active subunits, they can be used in artificial processes aimed at the conversion of solar energy into more useful energy forms (electricity or fuels)[3] or to store information.[4] Furthermore, if dendrimers contain a metal-based redox-active core surrounded by large organic branches, so mimicking biological sites such as cytochrome *c*, the electrochemical investigations can give information on the microenvironment experienced by the redox-active core and thus help to clarify the redox behavior of biological systems.[5]

[†] Università di Bologna.
[‡] E-mail: Roffia@ciam.unibo.it. Fax: (51)259456.
[§] Università di Messina.
[⊥] The University of Texas at Austin.
[∥] E-mail: ajbard@mail.utexas.edu. Fax: (512)471−0088.

(1) (a) Tomalia, D. A.; Naylor, A. M.; Goddard, W. A., III *Angew. Chem., Int. Ed. Engl.* **1990**, *29*, 138. (b) Fréchet, J. M. J. *Science* **1994**, *263*, 1710. (c) Bryce, M. R.; Devenport, W. In *Advances in Dendritic Macromolecules;* Newkome, G. R., Ed.; JAI: London, 1996; Vol. 3, p 115. (d) Newkome, G. R.; Moorefield, C. N.; Vögtle, F. *Dendritic Molecules. Concepts, Syntheses, Perspectives;* VCH: Weinheim, Germany, 1996. (e) Zeng, F.; Zimmerman, S. C. *Chem. Rev.* **1997**, *97*, 1681. (f) Peerlings, H. W. I.; Meijer, E. W. *Chem. Eur. J.* **1997**, *3*, 1563.

(2) (a) Ardoin, N.; Astruc, D. *Bull. Soc. Chim. Fr.* **1995**, *132*, 875. (b) Balzani, V.; Juris, A.; Venturi, M.; Campagna, S.; Serroni, S. *Chem. Rev.* **1996**, *96*, 759. (c) Constable, E. C. *Chem. Commun.* **1996**, 1073. (d) Achar, S.; Vittal, J. J.; Puddephatt, R. J. *Organometallics* **1996**, *15*, 43. (e) Liao, Y.-H.; Moss, J. R. *Organometallics* **1996**, *15*, 4307. (f) Huck, W. T. S.; Vanveggel, F. G. J. M.; Reinhoudt, D. N. *Angew. Chem., Int. Ed. Engl.* **1996**, *35*, 1213.

(3) (a) Balzani, V.; Campagna, S.; Denti, G.; Juris, A.; Serroni, S.; Venturi, M. *Sol. Energy Mater. Sol. Cells* **1995**, *38*, 159. (b) Balzani, V.; Campagna, S.; Denti, G.; Juris, A.; Serroni, S.; Venturi, M. *Acc. Chem. Res.* **1998**, *31*, 26.

(4) (a) Lehn, J.-M. *Supramolecular Chemistry*, VCH: Weinheim, Germany, 1995. (b) Astruc, D. *Acc. Chem. Res.* **1997**, *30*, 383. (c) Venturi, M.; Serroni, S.; Juris, A.; Campagna, S.; Balzani, V. *Top. Curr. Chem.*, in press.

(5) Dandliker, P. J.; Diederich, F.; Gisselbrecht, J.-P.; Louati, A.; Gross, M. *Angew. Chem., Int. Ed. Engl.* **1995**, *34*, 2725.

S0002-7863(98)00026-2 CCC: $15.00
Published on Web 05/23/1998

The properties of metal-based dendrimers depend to a large extent on the properties of their metal-based subunits.[4c] Well-known classes of luminescent and redox-active species are ruthenium(II) and osmium(II) polypyridine compounds;[6] therefore the choice of such compounds as components of photo- and redox-active dendrimers has been straightforward.

A big effort has been made to increase the number of metal-based subunits in dendritic complexes, and species containing tens of metal centers have been synthesized.[2,7] Most of the metal-based dendrimers reported can be considered as supramolecular systems; i.e., interactions between subunits are weak enough so that each unit maintains most of its specific properties and, at the same time, are strong enough so that new properties and intercomponent processes may arise.[2b,4c] In particular, photoinduced vectorial electron and energy transfer[2b,3,4c] can take place, and the direction of these processes (from the periphery of the system to the center or vice versa) can be predicted on the basis of the electrochemical and photophysical properties of the supermolecule and can be modulated by changing ligands and metal centers.

Knowledge of the electrochemical properties of metal-based dendrimers is therefore of paramount importance in understanding fully their properties and in foreseeing possible applications. For example, the study of successive metal-centered oxidations is important (i) for understanding the degree of metal−metal interaction within the dendritic array, (ii) for knowing which metal ion is easier to oxidize and therefore has the highest occupied d orbital, and (iii) for predicting the direction and the rate of a possible electron transfer. Furthermore, electrochemical data are useful for the photophysical characterization as they facilitate the assignment of metal-to-ligand-charge-transfer (MLCT) transitions on the basis of the known relation between spectroscopy and electrochemistry.[6b,8]

With this view, this work is aimed at studying the electrochemistry at very positive potentials in liquid SO_2 of Ru^{II} and Os^{II} dendritic polynuclear complexes (two hexanuclear species with a bis-chelating ligand as the core and one decanuclear species built around a metal core) and of several of their lower-nuclearity analogues, which can be considered as components of the larger dendritic species. The compounds investigated contain 2,3- or 2,5-bis(2-pyridyl)pyrazine (2,3- or 2,5-dpp) as bridging ligands and 2,2′-bipyridine (bpy) as terminal ligands (Chart 1). The choice of liquid SO_2 was dictated by the fact that this solvent together with a suitable supporting electrolyte, such as tetrabutylammonium hexafluoroarsenate ((TBA)AsF_6), offers the widest known anodic potential window.[9]

As discussed below, the identification of the redox sites for hexanuclear and decanuclear complexes was made possible by a bottom-up approach based on the comparison of their electrochemical behavior with that of mononuclear and dinuclear compounds.

Chart 1

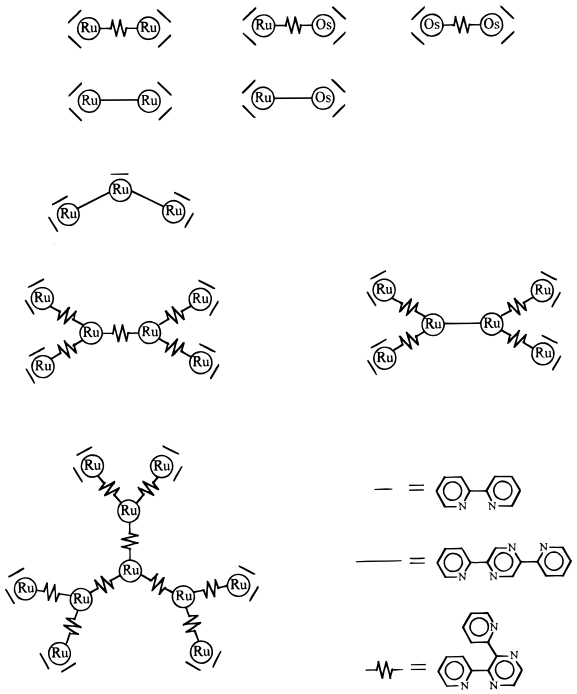

Experimental Section

Chemicals. All materials were reagent grade chemicals. Tetra-*n*-butylammonium hexafluoroarsenate was prepared from an aqueous solution of tetra-*n*-butylammonium bromide (Southwestern Analytical Chemicals, Austin, TX) to which an equivalent amount of aqueous lithium hexafluoroarsenate (Ozark-Mahoning, Pennwalt Corp., Tulsa, OK) was added. The resulting (TBA)AsF_6 crystals were filtered at 0 °C and redissolved in a minimal amount of hot ethyl acetate to which 10% (v/v) diethyl ether was added. The recrystallization was repeated twice, and the isolated product was dried under vacuum at 120 °C for 24 h (mp 245−246 °C). The synthesis of all of the investigated complexes has been reported previously.[10−14]

Procedure. The compound to be studied was weighed and placed in the cell with the supporting electrolyte, (TBA)AsF_6. The cell was placed on the vacuum line and heated with a silicone oil bath to 120 °C under vacuum (typically 9×10^{-6} to 2×10^{-5} mbar) for at least 24 h. Anhydrous SO_2 gas (99.99%) (Matheson Gas Products, Inc., Houston, TX) was purified by washing with concentrated sulfuric acid and percolated through a Woelm B-super 1 Alumina (Woelm Phara) column packed on glass wool. SO_2 was condensed into the cell at 77 K with a liquid nitrogen bath.

Apparatus. Electrochemical measurements were made with a CH Instruments (Memphis, TN) Model 660 electrochemical workstation. Cyclic voltammetric experiments were carried out in a single-compartment electrochemical cell utilizing a platinum disk (1.65 mm diameter) working electrode, a platinum wire counter electrode, and a silver spiral quasi-reference electrode (AgQRE) separated from the bulk solution by a fine frit. To measure the diffusion coefficient of the hexanuclear and decanuclear complexes, a 25-μm-diameter platinum ultramicroelectrode was used as the working electrode. We verified that the drift of the quasi-reference electrode was negligible for the time required for an experiment. Potentials given below are referenced

(6) (a) Meyer, T. J. *Pure Appl. Chem.* **1986**, *58*, 1193. (b) Juris, A.; Balzani, V.; Barigelletti, F.; Campagna, S.; Belser, P.; von Zelewsky, A. *Coord. Chem. Rev.* **1988**, *84*, 85. (c) Kalyanasundaram, K. *Photochemistry of Polypyridine and Porphyrin Complexes*; Academic Press: London, 1992.

(7) (a) Serroni, S.; Denti, G.; Campagna, S.; Juris, A.; Ciano, M.; Balzani, V. *Angew. Chem., Int. Ed. Engl.* **1992**, *31*, 1493. (b) Campagna, S.; Denti, G.; Serroni, S.; Juris, A.; Venturi, M.; Ricevuto, V.; Balzani, V. *Chem. Eur. J.* **1995**, *1*, 211.

(8) (a) Dodsworth, E. S.; Lever, A. B. P. *Chem. Phys. Lett.* **1989**, *124*, 152. (b) Curtis, J. C.; Sullivan, B. P.; Meyer, T. J. *Inorg. Chem.* **1983**, *22*, 224. (c) Ohsawa, Y.; Hanck, K. W.; De Armond, M. K. *J. Electroanl. Chem.* **1984**, *175*, 229.

(9) Garcia, E.; Kwak, J.; Bard, A. J. *Inorg. Chem.* **1988**, *27*, 4379.

(10) Denti, G.; Campagna, S.; Sabatino, L.; Serroni, S.; Ciano, M.; Balzani, V. *Inorg. Chem.* **1990**, *29*, 4750.

(11) Denti, G.; Serroni, S.; Sabatino, L.; Ciano, M.; Ricevuto, V.; Campagna, S. *Gazz. Chim. Ital.* **1991**, *121*, 37.

(12) Campagna, S.; Denti, G.; Sabatino, L.; Serroni, S.; Ciano, M.; Balzani, V. *Gazz. Chim. Ital.* **1989**, *119*, 415.

(13) Campagna, S.; Denti, G.; Serroni, S.; Ciano, M.; Balzani, V. *Inorg. Chem.* **1991**, *30*, 3728.

(14) (a) Serroni, S.; Denti, G.; Campagna, S.; Ciano, M.; Balzani, V. *J. Chem. Commun.* **1991**, 944. (b) Denti, G.; Campagna, S.; Serroni, S.; Ciano, M.; Balzani, V. *J. Am. Chem. Soc.* **1992**, *114*, 2944.

to an aqueous saturated calomel electrode (SCE) by measuring the AgQRE potential with respect to the 9,10-diphenylanthracene (DPA/DPA$^+$) couple.[9] Digital simulations were performed as described elsewhere.[15]

Determination of the Number of Electrons. The number of electrons corresponding to each electrochemical process is determined on the basis of a comparison between experimental and simulated curves, except for the first process of the two hexanuclear and the decanuclear complexes. The number of electrons (n) was determined from the value of the limiting current ($i_{lim} = 4nFDca$)[16] with a disk ultramicroelectrode (with radius $a = 12.5$ μm) and knowing the diffusion coefficient (D) of the electroactive species in a (TBA)AsF_6/acetonitrile solution from a chronoamperometric experiment ($D = 4.7 \times 10^{-6}$ cm^2/s for the two hexanuclear compounds and 3.1×10^{-6} cm^2/s for the decanuclear species). From a chronoamperogram obtained with a microdisk electrode of known radius (a), a direct determination of D independent of the number of electrons and the concentration of the electroactive species (c) is possible.[17] From an $i-t$ curve recorded over a time window which spans the transient and the steady-state regions, a plot of $i(t)/i_{lim}$ vs $t^{-1/2}$ yields a straight line with intercept 1 and slope S; $S = (\pi a^2/16D)^{1/2}$. From the value of S and the known a, D can be determined.

Results and Discussion

The electrochemical properties of the investigated ruthenium(II) and osmium(II) polypyridine complexes are discussed with the assumption that the ground and redox states can be represented with a sufficient degree of approximation by localized molecular orbitals.[4c,6] Redox processes can therefore be classified as metal- or ligand-centered.

The electrochemistry of the compounds reported here has been studied previously in acetonitrile at room temperature.[10−14,18−22] Under these experimental conditions, several ligand reductions were found, but only a few metal oxidations were observed due to the limited anodic potential window. In liquid SO_2, it has been reported[23,24] that the corresponding mononuclear homoleptic and heteroleptic compounds show both ligand-centered and metal-centered oxidations (one process for Ru^{II} complexes, Ru^{II}/Ru^{III} oxidation, and two processes for Os^{II} complexes, Os^{II}/Os^{III} and Os^{III}/Os^{IV} oxidations). Therefore the investigation of the electrochemistry of the title complexes at very positive potentials should significantly increase knowledge of the properties of metal-based dendrimers.

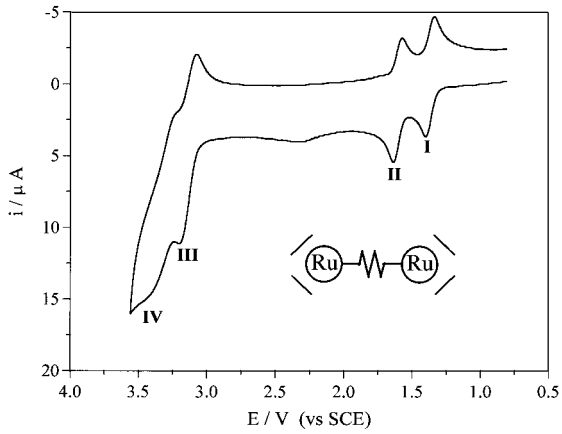

Figure 1. Cyclic voltammograms of 1.0 mM [(bpy)$_2$Ru(μ-2,3-dpp)-Ru(bpy)$_2$](PF$_6$)$_4$ in liquid SO_2/0.1 M (TBA)AsF_6 at −70 °C. Pt working electrode; sweep rate of 0.5 V/s.

Dinuclear Complexes. (a) Homometallic Ru^{II} Complexes. Figure 1 shows the electrochemical behavior of [(bpy)$_2$Ru(μ-2,3-dpp)Ru(bpy)$_2$]$^{4+}$ in liquid SO_2 at −70 °C. The first two peaks (I and II in Figure 1) correspond to two successive Nernstian and chemically reversible one-electron oxidations. Peaks III and IV are due to Nernstian two-electron transfers, and the last one presents a partial chemical irreversibility. The relative half-wave potentials, $E_{1/2}$, are reported in Table 1 along with those for mononuclear Ru and Os complexes previously studied[24] and for the other species investigated in this work.

The role of the bridging ligand in determining the electrochemical behavior of this dinuclear complex was investigated by comparison with the corresponding dinuclear species containing a 2,5-dpp bridge, [(bpy)$_2$Ru(μ-2,5-dpp)Ru(bpy)$_2$]$^{4+}$. This complex has electrochemical properties very close to those of [(bpy)$_2$Ru(μ-2,3-dpp)Ru(bpy)$_2$]$^{4+}$ (Table 1): two Nernstian and chemically reversible one-electron transfers followed, at more positive potentials, by two Nernstian and not completely reversible two-electron transfers. The last peak shows a higher degree of chemical irreversibility than the corresponding peak in [(bpy)$_2$Ru(μ-2,3-dpp)Ru(bpy)$_2$]$^{4+}$. However, the complex with the 2,5-dpp bridge shows an additional peak at very positive potentials, near base solution oxidation; this peak has an i_{pa} value much larger than the one-electron oxidation typified by the first peak. This behavior can be rationalized by a catalytic mechanism involving a species in high concentration like the solvent, and the contribution of the supporting electrolyte oxidation, since this peak is near the anodic limit of the (TBA)AsF_6/SO_2 system and this limit is due to the oxidation of the supporting electrolyte, not of the solvent.[9] This is a common feature for all the oxidations that occur near the anodic limit for the investigated dinuclear and polynuclear complexes and for the previously reported mononuclear species.[23,24]

(b) Homometallic Os^{II} Complex. A typical cyclic voltammogram for [(bpy)$_2$Os(μ-2,3-dpp)Os(bpy)$_2$]$^{4+}$ in liquid SO_2 at −70 °C is shown in Figure 2. Two doublets of peaks, due to Nernstian and chemically reversible one-electron transfers, are observed. When the potential is scanned to 4 V, another peak, very near to the anodic limit and therefore not well-resolved, is present. This peak is irreversible and has an i_{pa} value larger than the one-electron process typified by peak I.

(c) Heterometallic Ru^{II} and Os^{II} Complexes. Figure 3 shows the electrochemical behavior of [(bpy)$_2$Ru(μ-2,3-dpp)-Os(bpy)$_2$]$^{4+}$ in liquid SO_2 at −70 °C. Peaks I−III are Nernstian and chemically reversible one-electron oxidations. Upon scan-

(15) Paolucci, F.; Marcaccio, M.; Roffia, S.; Orlandi, G.; Zerbetto, F.; Prato, M.; Maggini, M.; Scorrano, G. *J. Am. Chem. Soc.* **1995**, *117*, 6572.
(16) *Microelectrodes: Theory and Applications*; Montenegro, M. I., Queiros, M. A., Daschbach, J. L., Eds.; Kluwer Dordrecht, The Netherlands, 1991.
(17) Denuault, G.; Mirkin, M. V.; Bard, A. J. *J. Electroanal. Chem.* **1991**, *308*, 27.
(18) (a) Wallace, A. W.; Murphy, W. R., Jr.; Petersen, J. D. *Inorg. Chim. Acta* **1989**, *166*, 47. (b) Braunstein, C. H.; Baker, A. D.; Strekas, T. C.; Gafney, H. D. *Inorg. Chem.* **1984**, *23*, 857. (c) Berger, R. M. *Inorg. Chem.* **1990**, *29*, 1920. (d) Fuchs, Y.; Lofters, S.; Dietter, T.; Shi, W.; Morgan, R.; Strekas, T. C.; Gafney, H. D.; Baker, A. D. *J. Am. Chem. Soc.* **1987**, *109*, 2691. (e) Haga, M.; Ali, M. M.; Koseki, S.; Yoshimura, A.; Nozaki, K.; Ohno, T. *Inorg. Chim. Acta* **1994**, *226*, 17. (f) Cooper, J. D.; MacQueen, D. B.; Petersen, J. D.; Wertz, D. W. *Inorg. Chem.* **1990**, *29*, 3701. (g) Molnar, S. M.; Nelville, K. R.; Jensen, G. E.; Brewer, K. J. *Inorg. Chim. Acta* **1993**, *206*, 69.
(19) Ernst, S. D.; Kaim, W. *Inorg. Chem.* **1989**, *28*, 1520.
(20) (a) Kalyanasundaram, K.; Nazeeruddin, Md. K. *Chem. Phys. Lett.* **1989**, *158*, 45. (b) Richter, M. M.; Brewer, K. J. *Inorg. Chem.* **1993**, *32*, 2827.
(21) Richter, M. M.; Brewer, K. J. *Inorg. Chem.* **1992**, *31*, 1594.
(22) Denti, G. Serroni, S.; Campagna, S.; Ricevuto V.; Juris, A.; Ciano, M.; Balzani, V. *Inorg. Chim. Acta* **1992**, *198−200*, 507.
(23) (a) Gaudiello, J. G.; Sharp, P. R.; Bard, A. J. *J. Am. Chem. Soc.* **1982**, *104*, 6373. (b) Gaudiello, J. G.; Norton, K. A.; Woodruff, W. H.; Bard, A. J. *Inorg. Chem.* **1984**, *23*, 3.
(24) Ceroni, P.; Paolucci, F.; Roffia, S.; Serroni, S.; Campagna, S.; Bard, A. J. *Inorg. Chem.*, in press.

Table 1. Half-Wave Potentials for the Ruthenium(II) and Osmium(II) Polypyridine Complexes Studied in Liquid SO_2 at −70 °C vs SCE[a]

complex	$E_{1/2}$, V				
	I	II	III	IV	V[b]
$[Ru(bpy)_2(2,3\text{-dpp})]^{2+}$ [c]	1.33	3.07	3.26	∼3.7[d]	
$[Ru(bpy)_2(2,5\text{-dpp})]^{2+}$ [c]	1.33	3.03	3.22	3.5[d]	
$[Os(bpy)_2(2,3\text{-dpp})]^{2+}$ [c]	0.94	2.56	3.6[d]	4.0[d]	
$[(bpy)_2Ru(\mu\text{-}2,3\text{-dpp})Ru(bpy)_2]^{4+}$	1.37	1.60	3.10[2]	∼3.3[2]	
$[(bpy)_2Ru(\mu\text{-}2,5\text{-dpp})Ru(bpy)_2]^{4+}$	1.37	1.60	3.16[2]	∼3.4[2]	∼4.2[d]
$[(bpy)_2Ru(\mu\text{-}2,5\text{-dpp})Os(bpy)_2]^{4+}$	0.98	1.56	2.66	3.2[2]	∼3.7[d]
$[(bpy)_2Ru(\mu\text{-}2,3\text{-dpp})Os(bpy)_2]^{4+}$	0.97	1.59	2.71	∼3.4[2][d]	
$[(bpy)_2Os(\mu\text{-}2,3\text{-dpp})Os(bpy)_2]^{4+}$	0.97	1.34	2.73	2.88	∼4.1[d]
$[(bpy)_2Ru(2,5\text{-dpp})Ru(bpy)(\mu\text{-}2,5\text{-dpp})Ru(bpy)_2]^{6+}$	1.41[2]	1.89	3.2[3]	3.4[2]	∼4.3[d]
$\{[(bpy)_2Ru(\mu\text{-}2,3\text{-dpp})]_2Ru(\mu\text{-}2,5\text{-dpp})Ru[(\mu\text{-}2,3\text{-dpp})Ru(bpy)_2]_2\}^{12+}$	1.44[4]	2.15[2]	3.2[4]	∼3.6[4][d]	∼4.2[d]
$\{[(bpy)_2Ru(\mu\text{-}2,3\text{-dpp})]_2Ru(\mu\text{-}2,3\text{-dpp})Ru[(\mu\text{-}2,3\text{-dpp})Ru(bpy)_2]_2\}^{12+}$	1.46[4]	2.11[2]	3.18[4]	3.4[4]	∼4.0[d]
$[Ru\{(\mu\text{-}2,3\text{-dpp})Ru[(\mu\text{-}2,3\text{-dpp})Ru(bpy)_2]_2\}_3]^{20+}$	1.46[6]	2.11[1]	2.44[3]	3.2[6]	3.5[d]

[a] Roman numbers I−V refer to the $E_{1/2}$, except as noted, for the different redox steps. The corresponding number of electrons is noted in square brackets [ ]. $E_{1/2}$ values were obtained either by directly averaging the cathodic and anodic peak potentials or by digital simulation. [b] The number of electrons corresponding to peak V is not reported because its determination is difficult due to a catalytic mechanism; see text. [c] Half-wave potentials reported in ref 24. For the sake of clarity, the redox processes involving a chemical modification of the mononuclear complexes[24] were omitted. [d] Anodic peak potentials, E_{pa}.

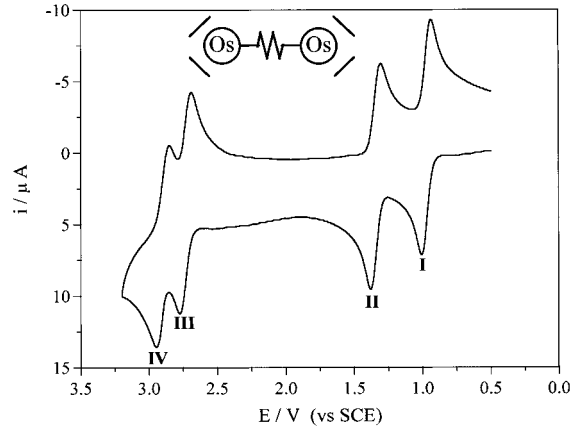

Figure 2. Cyclic voltammograms of 2.1 mM $[(bpy)_2Os(\mu\text{-}2,3\text{-dpp})Os(bpy)_2](PF_6)_4$ in liquid SO_2/0.1 M $(TBA)AsF_6$ at −70 °C. Pt working electrode; sweep rate of 0.5 V/s.

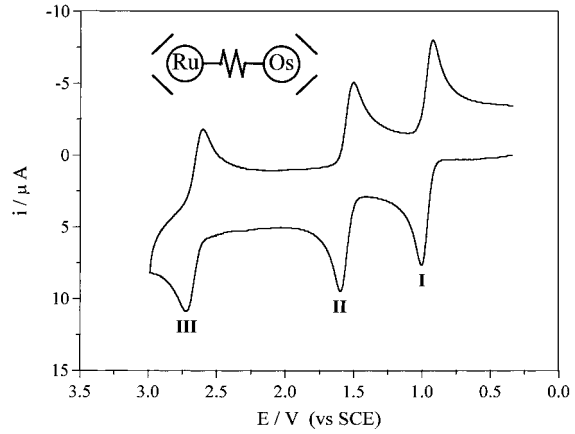

Figure 3. Cyclic voltammograms of 2.2 mM $[(bpy)_2Ru(\mu\text{-}2,3\text{-dpp})Os(bpy)_2](PF_6)_4$ in liquid SO_2/0.1 M $(TBA)AsF_6$ at −70 °C. Pt working electrode; sweep rate of 0.5 V/s.

ning the potential to more positive values, another peak appears corresponding to a two-electron and chemically irreversible process.

The heterometallic dinuclear analogue with 2,5-dpp as the bridging ligand shows a very similar electrochemical behavior (Table 1), except for the presence of one more process at very positive potentials ($E_{pa} \approx 3.7$ V) with a value of i_{pa} larger than that expected for a two-electron process. This behavior parallels that observed in the case of homometallic Ru dinuclear

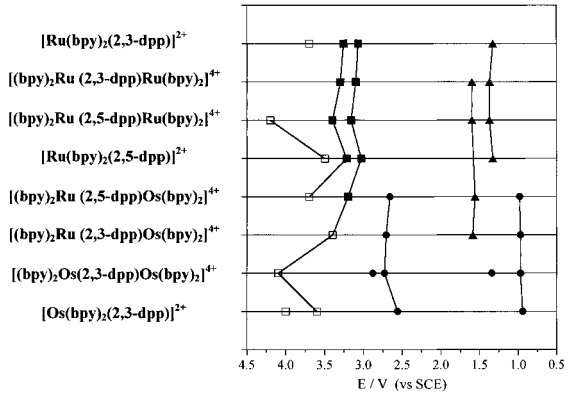

Figure 4. Comparison of the redox potentials for the dinuclear complexes studied in 0.1 M $(TBA)AsF_6/SO_2$ at −70 °C and the previously reported mononuclear analogues.[24] $E_{1/2}$ values for Ru (▲), Os (●), and ligand oxidations (■) and E_{pa} values for ligand oxidations at very positive potentials (□). For the sake of clarity, the redox processes involving a chemical modification of the mononuclear complexes[24] have been omitted.

complexes (vide supra); i.e., the complex containing the 2,5-dpp bridge shows one more peak than the one with a 2,3-dpp bridging ligand.

(d) Location of the Redox Sites in the Investigated Dinuclear Complexes. The identification of the redox sites in the dinuclear complexes was based on a comparison with the corresponding mononuclear species $[M^{II}(bpy)_n(dpp)_{3-n}]$, where $M^{II} = Ru^{II}$ or Os^{II} and $n = 0$, 2, or 3 (Figure 4).[24] In these mononuclear compounds (i) metal-centered and ligand-centered oxidations occur in two distinct potential regions, the former below 3 V and the latter above 3 V, and (ii) Ru mononuclear complexes show one metal-centered oxidation (Ru^{II}/Ru^{III}), while Os analogues present two metal-based processes (Os^{II}/Os^{III} and Os^{III}/Os^{IV}). Analogous behavior can be assumed for the dinuclear complexes on the basis of the occurrence of two, three, and four successive one-electron transfers below 3 V for $[(bpy)_2Ru(\mu\text{-dpp})Ru(bpy)_2]^{4+}$, $[(bpy)_2Ru(\mu\text{-dpp})Os(bpy)_2]^{4+}$, and $[(bpy)_2Os(\mu\text{-}2,3\text{-dpp})Os(bpy)_2]^{4+}$, respectively. The following discussion is also consistent with the electrochemical data previously reported in acetonitrile.[10,11,18−21]

(e) Metal-Centered Processes. Peak I for both $[(bpy)_2Ru(\mu\text{-}2,3\text{-dpp})Ru(bpy)_2]^{4+}$ (Figure 1) and $[(bpy)_2Ru(\mu\text{-}2,5\text{-dpp})Ru(bpy)_2]^{4+}$ occurs in the same potential region but is slightly more positively displaced than the first metal-centered process

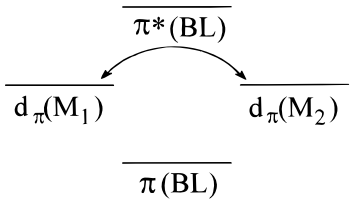

Figure 5. Orbital energy diagram illustrating superexchange interaction between two metal ions (M_1 and M_2) through a bridging ligand (BL). $d_\pi(M_1)$, $d_\pi(M_2)$, π(BL), and π^*(BL) represent orbitals of the two metal centers and the LUMO and HOMO of the bridging ligand, respectively.

for the mononuclear analogues $[Ru(2,3\text{-dpp})(bpy)_2]^{2+}$ and $[Ru(2,5\text{-dpp})(bpy)_2]^{2+}$ (Figure 4). Therefore, peak I can be assigned to the oxidation of one of the two Ru ions. Peak II is necessarily ascribed to the second Ru ion oxidation. The splitting between the two metal-centered oxidations and the positive displacement of the first metal oxidation with respect to the mononuclear analogues are common features for all of the investigated dinuclear complexes and reflect the extent of metal−metal interaction through the bridge.[25] In a pictorial and simplified view the dinuclear complexes $[(bpy)_2M^{II}(\mu\text{-BL})M^{II}(bpy)_2]^{4+}$ can be seen as mononuclear $[M^{II}(bpy)_2(BL)]^{2+}$ species carrying the electron-acceptor $[M^{II}(bpy)_2]^{2+}$ substituent on the bridging ligand (BL).[13] The electron donation from μ-BL to the substituent causes a depletion of negative charge on the BL and therefore the transfer of some electronic charge from the first metal center to μ-BL; as a consequence, the metal oxidation is displaced to more positive values. This effect will be strongly enhanced when the $[M^{II}(bpy)_2]^{2+}$ unit is coupled to the strong electron-accepting $[M^{III}(bpy)_2]^{3+}$ unit, thus explaining the separation between the two successive oxidations of the Ru ions.

A more rigorous description of metal−metal interaction via the bridge can be attempted on the basis of the superexchange theory,[25,26] where the overlap between metal orbitals is mediated by overlap with those of the bridging ligand. Two different modes of metal−metal communication through a bridge are possible: (i) an electron-transfer mode across low-lying π^*_{BL} orbitals and (ii) a hole transfer mode across occupied π_{BL} orbitals. For complexes having low-lying π^*_{BL} orbitals, such as 2,3- and 2,5-dpp, mode i is the dominant one.[25] In this case, metal−metal interaction depends on the energy gap between the d_π-metal orbitals and the LUMO bridging ligand orbitals (see Figure 5). The double coordination of BL lowers the π^*_{BL} orbital (in fact, a large positive shift for the first reduction of the bridging ligand between mono- and dinuclear species is reported[10]), so it can couple more efficiently with d_π-metal orbitals as compared to the mononuclear analogues. Therefore, stabilization of d_π-metal orbitals via back-bonding can explain the observed positive shift of the first metal-centered oxidation in dinuclear complexes with respect to mononuclear analogues. Electrostatic interaction between charged metal centers may in part play a role. The relative importance of through-bond and Coulombic interactions is, however, difficult to estimate in the presence of counterions, which can effectively diminish the latter.[27] Indications in this regard come, however, from considering the case of Os−Os dinuclear complexes (vide infra).

For $[(bpy)_2Os(\mu\text{-}2,3\text{-dpp})Os(bpy)_2]^{4+}$ the first doublet (peaks I and II in Figure 2) corresponds to the oxidation of the two Os ions from Os^{II} to Os^{III} and the second doublet (peaks III and IV) from Os^{III} to Os^{IV}. This assignment is supported by (i) the fact that peaks I and III are close to, although positively shifted from (especially peak III), the first two processes shown by $[Os(2,3\text{-dpp})(bpy)_2]^{2+}$ and attributed to successive one-electron oxidation of the Os ion[24] and (ii) the previously reported data on the electrochemistry of this complex in acetonitrile,[11,20] although in this solvent only the first doublet is observed because of the narrower potential window.

The separation within the first doublet is greater than the separation within the second, indicating that the metal−metal interaction is lower for the second doublet. This result cannot be explained on the basis of pure Coulombic interactions, as mentioned above. Probably through-bond interaction dominates the energetics of the successive oxidation of the present species. In fact, the energy gap between the d_π-metal orbitals and the π^*_{BL} orbital is expected to be lower for the second doublet of $[(bpy)_2Os(\mu\text{-}2,3\text{-dpp})Os(bpy)_2]^{4+}$ than for the first because the first oxidation of the two metal ions stabilizes the d_π-metal orbitals and enhances the energy gap between these orbitals and the π^*_{BL} orbital. According to the superexchange theory, this explains the diminished metal−metal interaction for the second doublet. Finally, the distance between the first two peaks is larger than the corresponding one between the two Ru oxidations in $[(bpy)_2Ru(\mu\text{-}2,3\text{-dpp})Ru(bpy)_2]^{4+}$. Indeed, the higher energy of the d_π orbitals of the Os ions allows a more efficient mixing of these orbitals with the π^*_{BL} orbital.[20b,25] This also confirms that for the investigated complexes metal−metal interaction occurs across low-lying π^*_{BL} orbitals and not across the occupied π_{BL} orbitals. In the latter case, in fact, the greatest degree of interaction should be in the Ru complexes since the Ru d_π orbitals are nearer to the occupied π_{BL} orbitals.

For $[(bpy)_2Ru(\mu\text{-}2,3\text{-dpp})Os(bpy)_2]^{4+}$ and $[(bpy)_2Ru(\mu\text{-}2,5\text{-dpp})Os(bpy)_2]^{4+}$ peaks I and III occur at almost the same potential as peaks I and III of $[(bpy)_2Os(\mu\text{-}2,3\text{-dpp})Os(bpy)_2]^{4+}$ (Figure 4), corresponding to Os^{II}/Os^{III} and Os^{III}/Os^{IV} oxidations of the first Os center, while the peak II potential is very close to that of peak II for $[(bpy)_2Ru(\mu\text{-}2,3\text{-dpp})Ru(bpy)_2]^{4+}$, due to Ru^{II}/Ru^{III} oxidation of the second metal center. Therefore, peaks I, II, and III correspond to Os^{II}/Os^{III}, Ru^{II}/Ru^{III}, and Os^{III}/Os^{IV} oxidations, respectively.

Finally, comparison between $[(bpy)_2Ru(\mu\text{-}2,3\text{-dpp})Ru(bpy)_2]^{4+}$ and $[(bpy)_2Ru(\mu\text{-}2,5\text{-dpp})Ru(bpy)_2]^{4+}$ on one hand and between $[(bpy)_2Ru(\mu\text{-}2,3\text{-dpp})Os(bpy)_2]^{4+}$ and $[(bpy)_2Ru(\mu\text{-}2,5\text{-dpp})Os(bpy)_2]^{4+}$ on the other shows that metal oxidations take place at the same potential within each couple (Figure 4). Therefore, the degree of metal−metal interaction is not strongly affected by the different geometry of the two bridges (μ-2,5-dpp is planar, while μ-2,3-dpp is slightly distorted from a planar geometry because of the steric hindrance between the two pyridine rings[10]), as found previously for the corresponding

(25) Giuffrida, G.; Campagna, S. *Coord. Chem. Rev.* **1994**, *135/136*, 517.
(26) (a) Halpern, J.; Orgel, L. E. *Discuss Faraday Soc.* **1960**, *29*, 32. (b) McConnell, H. M. *J. Chem. Phys.* **1961**, *35*, 508. (c) Day, P. *Comments Inorg. Chem.* **1981**, *1*, 155. (d) Miller, J. R.; Beitz, J. V. *J. Chem. Phys.* **1981**, *74*, 6746. (e) Richardson, D. E.; Taube, H. *J. Am. Chem. Soc.* **1983**, *105*, 40. (f) Newton, M. D. *Chem. Rev.* **1991**, *91*, 767. (g) Jordan, K. D.; Paddon-Row: M. N. *Chem. Rev.* **1992**, *92*, 395. (h) Todd, M. A.; Nitzan, A.; Ratner, M. A. *J. Phys. Chem.* **1993**, *97*, 29.

(27) (a)The Coulombic interaction in a vacuum is expected to be about 4.4 eV for the species $[(bpy)_2M^{II}(\mu\text{-dpp})M^{III}(bpy)_2]^{5+}$, considering a distance of 6.5 Å between the two metal centers (estimated from molecular models). However, the effect of solvent, counterions, and formation of ion pairing should be taken into account, as already pointed out in the literature.[27b] The larger splitting in liquid SO_2 compared to acetonitrile solution between the first two metal-centered oxidations for the homometallic dinuclear complexes investigated (230 vs 170 mV for $[(bpy)_2Ru(\mu\text{-}2,3\text{-dpp})Ru(bpy)_2]^{4+}$ and 370 vs 300 mV for $[(bpy)_2Os(\mu\text{-}2,3\text{-dpp})Os(bpy)_2]^{4+}$) demonstrates that the effect of counterions and ion pairing is not very important. In fact, this effect should be stronger in liquid SO_2 since its dielectric constant is lower than that of acetonitrile. (b) El-Kasmi, A.; Lexa, D.; Maillard, P.; Momenteau, M.; Savéant, J.-M. *J. Phys. Chem.* **1993**, *97*, 6090.

homometallic Os complexes.[24] Finally, it is well-known that dpp ligands allow metal−metal communication as demonstrated by the observation of internal intervalence bands in the mixed valence species for $[(bpy)_2Os(\mu\text{-}2,3\text{-}dpp)Os(bpy)_2]^{4+}$ and $[(bpy)_2Os(\mu\text{-}2,3\text{-}dpp)Ru(bpy)_2]^{4+}$;[20b] although, in ref 20b electrostatic and solvation effects are suggested to contribute to the energy level of the mixed valence species.

(f) Ligand-Centered Oxidations. For all of the investigated dinuclear complexes, the first ligand-based processes probably involve bpy's rather than bridging ligands on the basis of analogous behavior of the previously reported mononuclear compounds.[24] Furthermore, in the complexes studied here, each bridging ligand is linked to two positively charged metal subunits, so the dpp π orbitals are more stabilized than the corresponding bpy orbitals.

Peaks III and IV for $[(bpy)_2Ru(\mu\text{-}2,3\text{-}dpp)Ru(bpy)_2]^{4+}$ (Figure 1) and $[(bpy)_2Ru(\mu\text{-}2,5\text{-}dpp)Ru(bpy)_2]^{4+}$ are only slightly positively displaced with respect to the mononuclear analogues, and they can be ascribed to bpy oxidations. In particular, each one of the two-electron processes (peaks III and IV) involves two bpy's coordinated to the two different metal centers since the interaction between bpy's bonded to different metal centers is predicted to be much lower (experimentally not appreciable in this case) than that between bpy's coordinated to the same Ru ion. In the negative potential region, the behavior is different.[18c,f,28] In $[(bpy)_2Ru(\mu\text{-}2,3\text{-}dpp)Ru(bpy)_2]^{4+}$, for example, successive reductions of bpy's coordinated to different metal centers result in better-resolved peaks with $\Delta E_{1/2} \geq 60$ mV. This different behavior can be rationalized as follows. Bpy's are reduced when the metal is in its +2 oxidation state, and when bpy's are oxidized, they are coordinated to Ru^{III} ions since bpy oxidation occurs after Ru oxidation. Therefore, in the latter case, the d_π orbitals are lowered in energy and the interaction between the two Ru^{III} ions through the π^*_{BL} orbital, and as a consequence between bpy's bonded to different metal centers, is smaller. On the other hand, the communication between bpy's coordinated to the same metal center (measured from the splitting between the second and the third bpy-centered peaks in the cathodic region and the separation between peaks III and IV of Figure 1 in the anodic region) is only slightly smaller in oxidation ($\Delta E_{1/2} = 200$ mV in oxidation vs $\Delta E_{1/2} = 230$ mV in reduction).

For $[(bpy)_2Ru(\mu\text{-}2,5\text{-}dpp)Ru(bpy)_2]^{4+}$, another peak ($E_{pa} \approx 4.2$ V) appears after the bpy oxidations. This peak can be assigned to the bridge oxidation and is very positively shifted in comparison with the mononuclear analogue.[29] In fact, the presence of two, instead of one, electron-withdrawing $[Ru^{III}(bpy^{\cdot+})_2]^{5+}$ units in the dinuclear complex makes the bridge more difficult to oxidize. This peak is not observed for $[(bpy)_2Ru(\mu\text{-}2,3\text{-}dpp)Ru(bpy)_2]^{4+}$ even if the potential is scanned to the anodic limit. This behavior is consistent with the observation that 2,3-dpp is oxidized at a more positive potential than 2,5-dpp in the mononuclear species.[24] Therefore, the bridge oxidation is beyond the available potential window for $[(bpy)_2Ru(\mu\text{-}2,3\text{-}dpp)Ru(bpy)_2]^{4+}$.

For $[(bpy)_2Os(\mu\text{-}2,3\text{-}dpp)Os(bpy)_2]^{4+}$, after the four metal-based oxidations, only one irreversible peak at about 4.1 V is observed. This peak is probably due to the oxidation of two bpy's bonded to the two different Os ions, although it is difficult to evaluate the number of electrons involved since the peak is poorly resolved. This peak occurs at a much more positive potential than in the homometallic Ru analogue because of the higher charge of the complex. In fact, in the Os complex each bpy coordinates to a $[M^{IV}(bpy)(BL)]^{4+}$ unit, while in the Ru complex it is bonded to a $[M^{III}(bpy)(BL)]^{3+}$ unit.

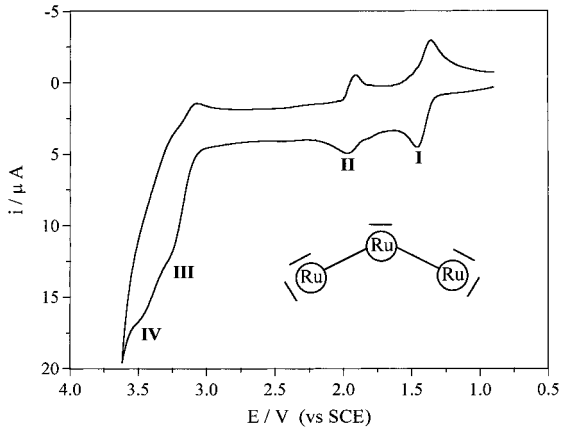

Figure 6. Cyclic voltammograms of 0.6 mM $[(bpy)_2Ru(\mu\text{-}2,5\text{-}dpp)Ru(bpy)(\mu\text{-}2,5\text{-}dpp)Ru(bpy)_2](PF_6)_6$ in liquid SO_2/0.1 M $(TBA)AsF_6$ at −70 °C. Pt working electrode; sweep rate of 0.2 V/s.

As in the previous assignments for the two heterometallic complexes, the fourth peak involves two bpy's coordinated to different metal centers and the fifth peak of $[(bpy)_2Ru(\mu\text{-}2,5\text{-}dpp)Os(bpy)_2]^{4+}$, not observed in $[(bpy)_2Ru(\mu\text{-}2,3\text{-}dpp)Os(bpy)_2]^{4+}$, is due to the oxidations of the second pair of bpy's.

Thus for the Ru−Ru, Ru−Os, and Os−Os dinuclear complexes studied, the ligand oxidations take place at increasingly positive potentials (Figure 4) as a result of the higher positive charge of Os^{IV} compared to Ru^{III}.

Dendritic Polynuclear Complexes. Complexes containing 3, 6, and 10 Ru^{II} ions were investigated; the gradual increase of the nuclearity was of paramount importance for understanding the electrochemical behavior of the more complex compounds. For this reason we also include here a discussion of the trinuclear species, which cannot be strictly considered as a dendrimer.

A typical cyclic voltammogram for $[(bpy)_2Ru(\mu\text{-}2,5\text{-}dpp)Ru(bpy)(\mu\text{-}2,5\text{-}dpp)Ru(bpy)_2]^{6+}$ in liquid SO_2 at −70 °C is shown in Figure 6. Peaks I and II correspond to Nernstian and chemically reversible two- and one-electron transfers, respectively. Peaks III and IV present a partial degree of chemical irreversibility and they are not well-resolved, but they correspond to successive three- and two-electron transfers. If the potential is scanned to the anodic limit, another irreversible peak at about 4.3 V (Table 1) is present with an i_{pa} value much larger than the two-electron transfer typified by peak I.

In the following discussion, attention will be focused on the processes involving Ru ions, while those relative to ligand oxidations will be discussed in a separate section.

Peaks I and II for $[(bpy)_2Ru(\mu\text{-}2,5\text{-}dpp)Ru(bpy)(\mu\text{-}2,5\text{-}dpp)Ru(bpy)_2]^{6+}$ occur in the potential region of metal oxidations; in particular, peak I is close to the first peak of $[(bpy)_2Ru(\mu\text{-}2,5\text{-}dpp)Ru(bpy)_2]^{4+}$, while peak II is significantly positively shifted with respect to the second peak of the dinuclear analogue. Therefore, the bielectronic peak I can be assigned to the two external Ru ions and the monoelectronic peak II to the central Ru. This assignment of the redox sites is consistent with that reported in acetonitrile,[10,12] although in that case the second process was not resolved because it was too close to the anodic limit.

Very similar electrochemical properties were observed for the two hexanuclear compounds, $\{[(bpy)_2Ru(\mu\text{-}2,3\text{-}dpp)]_2Ru$-

(28) Roffia, S. et al. Work in preparation.

(29) Although these peaks are chemically irreversible, a comparison of E_{pa} values may be done since the kinetic parameters for the chemical reactions following electron transfers are probably similar.

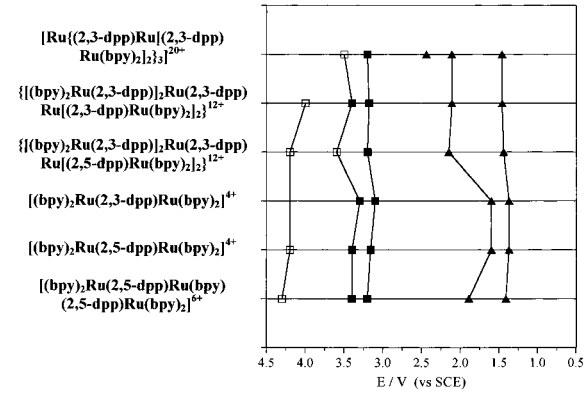

Figure 7. Comparison of the redox potentials for the polynuclear and dinuclear complexes studied in liquid SO_2/0.1 M (TBA)AsF_6 at −70 °C. $E_{1/2}$ values for metal oxidations (▲) and ligand oxidations (■) and E_{pa} values for ligand oxidations at very positive potentials (□).

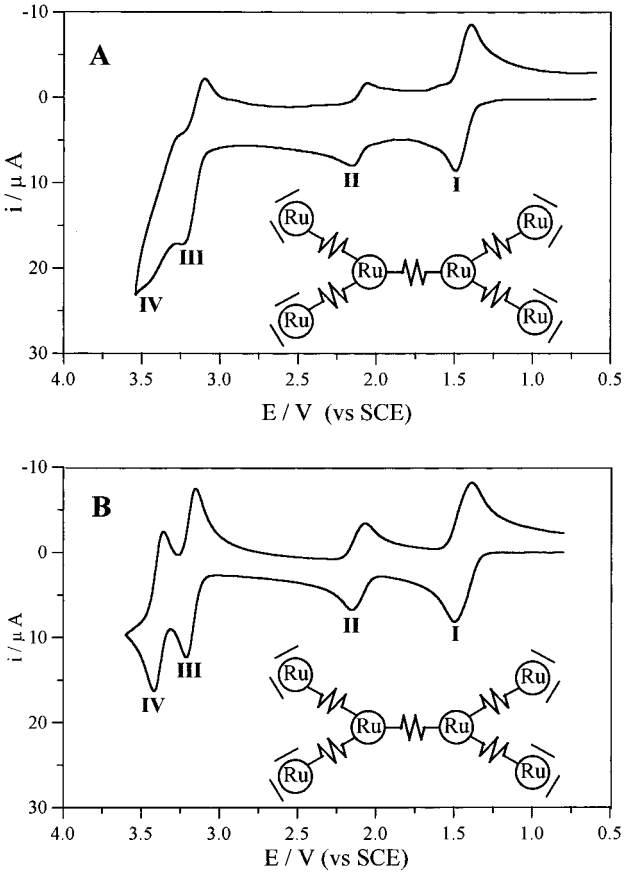

Figure 8. Cyclic voltammograms of 0.6 mM {[(bpy)$_2$Ru(μ-2,3-dpp)]$_2$Ru(μ-2,3-dpp)Ru[(μ-2,3-dpp)Ru(bpy)$_2$]$_2$}$(PF_6)_{12}$ in liquid SO_2/0.1 M (TBA)AsF_6 at −70 °C. Pt working electrode; sweep rate of 0.2 V/s.

(μ-2,3-dpp)Ru[(μ-2,3-dpp)Ru(bpy)$_2$]$_2$}$^{12+}$ and {[(bpy)$_2$Ru(μ-2,3-dpp)]$_2$Ru(μ-2,5-dpp)Ru[(μ-2,3-dpp)Ru(bpy)$_2$]$_2$}$^{12+}$ (Figure 7). The electrochemical behavior in liquid SO_2 of the former is presented in Figure 8. Within the reported potential window, four peaks are observed corresponding, respectively, to Nernstian four-, two-, four-, and four-electron transfers; peak IV presents a partial degree of chemical irreversibility. Scanning the potential to more positive values than in Figure 8, one more peak is observed (E_{pa} = 4.2 V; Table 1) with an i_{pa} value much larger than peak I.

In the two hexanuclear complexes, peak I involves the four external Ru ions and peak II is due to the two internal ones

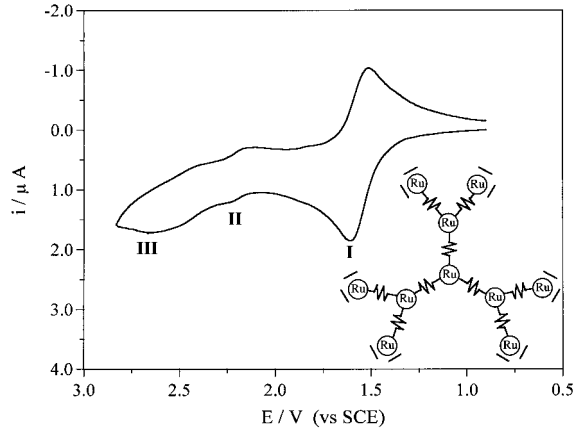

Figure 9. Cyclic voltammograms of 0.8 mM [Ru{(μ-2,3-dpp)Ru[(μ-2,3-dpp)Ru(bpy)$_2$]$_2$}$_3$]$(PF_6)_{20}$ in liquid SO_2/0.1 M (TBA)AsF_6 at −70 °C. Pt working electrode; sweep rate of 0.1 V/s.

(for the determination of the number of electrons, see the Experimental Section). This attribution is based on the fact that central metals are bonded to three (instead of one) of the 2,3- or 2,5-dpp ligands, which have a stronger back-bonding power than bpy ligands (π*-dpp orbitals are lower than π*-bpy ones), and therefore the inner metals are more difficult to oxidize than peripheral ones. The first four-electron transfer was previously observed in acetonitrile.[13,22] The experimental observation that the oxidation of the two internal centers occurs at the same potential was not expected on the basis of the behavior of the dinuclear complexes, [(bpy)$_2$Ru(μ-2,3-dpp)Ru(bpy)$_2$]$^{4+}$ and [(bpy)$_2$Ru(μ-2,5-dpp)Ru(bpy)$_2$]$^{4+}$, in which the two Ru^{II} oxidations occur at distinct potentials ($\Delta E_{1/2}$ = 230 mV). The interaction between the two central metals in the hexanuclear complexes must be much smaller than in the corresponding dinuclear complexes, contrary to what is predicted on the basis of electrostatic repulsion. To explain this experimental observation, we can represent the two four-electron oxidized hexanuclear and the dinuclear complexes as [R_2Ru(μ-dpp)RuR_2]$^{n+}$, where R = $[Ru^{III}(2,3\text{-dpp})(bpy)_2]^{3+}$ and bpy, respectively. The extent of metal−metal interactions is clearly a function of the peripheral group R. In the two four-electron oxidized hexanuclear compounds, the four very electron-withdrawing peripheral groups $[Ru^{III}(2,3\text{-dpp})(bpy)_2]^{3+}$ cause a lowering of the d_π orbitals of the two central Ru^{II} ions and therefore a lower overlap between metal-d_π and π^*_{BL} orbitals (Figure 5) than in the dinuclear analogues. This results in a smaller interaction between the two central Ru ions and in virtually coincident oxidation potentials.[30] The strong lowering of the d_π orbitals of the central Ru ions is also demonstrated by the larger distance between peaks I and II in the hexanuclear complex than in the dinuclear complex (Figure 7).

The cyclic voltammogram of the decanuclear complex [Ru{(μ-2,3-dpp)Ru[(μ-2,3-dpp)Ru(bpy)$_2$]$_2$}$_3$]$^{20+}$ (Figure 9) shows a six-electron process (peak I) followed by two broad and not completely reversible peaks (II and III). This partial irreversibility is due to the presence of water in the sample because water is irreversibly oxidized in the same potential region.[31] Upon scanning the potential to more positive values, two more

(30) The metal−metal interaction between the two inner Ru^{II} ions in the hexanuclear complexes in the ground state (that is, before oxidation of the peripheral units) is expected to be intermediate between the interaction in [(bpy)$_2$Ru(μ-dpp)Ru(bpy)$_2$]$^{4+}$ and peripherally oxidized hexanuclear compounds. The value of such an interaction is not available from the experiments described here.

(31) It is difficult to eliminate this water since it is inside the solid state and heating above 100 °C can decompose the compound.

peaks at very positive potentials are observed. They are not completely reversible and are very poorly defined; an estimate of the corresponding number of electrons is therefore not possible. On the basis of symmetry considerations, three electrochemically nonequivalent sets of metal centers are expected: (i) the six peripheral Ru ions not strongly interacting with each other (since they are not connected through a common bridging ligand); (ii) the three equivalent Ru ions directly linked to the central one; and (iii) the central Ru. According to this view, a six-electron process centered on the peripheral Ru ions is predicted, followed by a one-electron process due to the central Ru (the central ion is easier to oxidize than the remaining three Ru ions because it is not directly linked to the peripheral oxidized Ru^{III} ions) and finally a three-electron process involving the remaining three Ru centers. Peak I (Figure 9) is shown to correspond to a six-electron transfer (see Experimental Section). Peaks II and III are broad and not completely reversible, and the determination of the corresponding number of electrons is therefore difficult, but the simulation supports this assignment.

In all of the polynuclear complexes studied, the first and second metal oxidations occur at more positive potentials than in the corresponding dinuclear complexes (Table 1). This is due to the higher charge of the polynuclear compounds and to the presence in the high-nuclearity compounds of more electron-withdrawing substituents linked to the inner metals than those of the dinuclear complexes.

(a) Ligand-Centered Oxidations. Less emphasis will be given to the processes occurring above 3 V; in most cases, they are irreversible and poorly resolved. These processes can be attributed to ligand-centered oxidations on the basis of the analogous behavior of the investigated dinuclear complexes.

For all of the investigated polynuclear complexes, metal-based oxidations are followed by oxidations of bpy ligands on the basis of the same considerations given for the dinuclear compounds (vide supra). Therefore, peaks III and IV of $[(bpy)_2Ru(\mu\text{-}2,5\text{-}dpp)Ru(bpy)(\mu\text{-}2,5\text{-}dpp)Ru(bpy)_2]^{6+}$ (Figure 6) and of the two hexanuclear complexes (Figure 8 and Table 1) and the fourth and fifth peaks for the decanuclear complex ($E_{1/2}$ = 3.2 V; E_{pa} = 3.5 V) can be ascribed to bpy oxidations. In particular, for the two hexanuclear complexes and the decanuclear one, metal-centered oxidations are followed by two processes; each corresponds to the oxidation of bpy's bonded to the different external Ru ions (four-electron peaks for the first two species and six-electron peaks for the last one). As with the dinuclear complexes, bpy's coordinated to different metal centers are not appreciably interacting, while bpy's bonded to the same metal center interact with each other through the metal and therefore are oxidized at distinct potentials. The trinuclear complex peak III (Figure 6) involves the three bpy's bonded to the different Ru ions. The bpy coordinated to the central Ru ion, which has a lower electron density than the external ones, was expected to be oxidized at a slightly more positive potential than the other two bpy's, but no appreciable shift was observed experimentally. Peak IV is attributed to the remaining two bpy's. For the trinuclear and hexanuclear species another ligand oxidation takes place at very positive potentials (E_{pa} = 4.3 and 4.2 V, respectively) and it likely involves the bridging ligand.

Conclusions

The electrochemical study in liquid SO_2 at −70 °C of dinuclear and dendritic polynuclear Ru^{II} and Os^{II} complexes containing 2,3- and 2,5-dpp as bridging ligands and bpy as terminal ligands has allowed the observation of several metal- and ligand-centered oxidations (to ∼4.3 V) previously inaccessible. The following order of oxidations is observed for polynuclear species: peripheral metal centers < inner metal centers < bpy ligands < 2,3- or 2,5-dpp bridges.

The identification of the redox sites for hexanuclear and decanuclear complexes was made possible by a bottom-up approach based on comparison of their electrochemical behavior with that of the simpler mononuclear and dinuclear compounds.

This study has allowed, for the first time, the observation of (i) both Os (Os^{II}/Os^{III} and Os^{III}/Os^{IV}) oxidations in $[(bpy)_2Os(\mu\text{-}2,3\text{-}dpp)Os(bpy)_2]^{4+}$, $[(bpy)_2Ru(\mu\text{-}2,3\text{-}dpp)Os(bpy)_2]^{4+}$, and $[(bpy)_2Ru(\mu\text{-}2,5\text{-}dpp)Os(bpy)_2]^{4+}$; (ii) oxidations of the inner Ru ions in the investigated trinuclear, hexanuclear, and decanuclear complexes; and (iii) bpy and 2,3- or 2,5-dpp oxidations occurring at very positive potentials (>3 V). The first observation is useful in understanding the lowering in metal−metal communication going from Os^{II} to Os^{III} ions due to the increased energy gap between π^*_{BL} and metal-d_π orbitals, as a consequence of the removal of an electron from each metal center. Inner Ru ion oxidations give information on the extent of metal−metal interaction and electrochemical equivalency between different metal centers in dendrimers made of metal-based subunits. In particular, for the two hexanuclear compounds, we found that, after the oxidation of the four peripheral Ru ions, the communication between the two central Ru^{II} ions becomes too low to be observed in a cyclic voltammogram. Therefore, after a four-electron process, a two-electron oxidation is observed, rather than the two one-electron oxidations expected on the basis of the behavior of the dinuclear complexes. On the other hand, the decanuclear complex exhibits three distinct sets of metal-centered oxidations due to the six peripheral ions, the central one, and the remaining three inner metals. Analysis of ligand-based processes allowed deduction of the order of the relative energy levels of the occupied ligand-π orbitals on the basis of the corresponding order of oxidation.

The oxidation pattern in these compounds depends on the nature of the metals (Ru or Os) and on their specific positions in the arrays (topology). Therefore, their oxidation patterns can be viewed as a sort of *fingerprint* of each particular dendrimer. This demonstrates that the redox properties can also be used as a powerful tool for the chemical characterization of large and highly charged supermolecules.

Acknowledgment. We thank Dr. Jeff Debad and Prof. Vincenzo Balzani for fruitful discussions. This work was partly supported by MURST, CNR, and the University of Bologna (Funds for Selected Topics) and the National Science Foundation (Grant CHE 9508525). P. C. thanks NATO for a grant (No. 9612/71, Supramolecular Chemistry Special Programme) which allowed her to work in Austin.

JA980026E